Boundary Friction of Sliding Surfaces Under the Heavy Load (1st Report)

Boundary Friction of Sliding Surfaces Under the Heavy Load (1st Report)

Yoshio WATANABE* and Tokio SASAKI**

(Received Nov. 30, 1962)

This paper presents the results of the investigation carried out to compare the frictional properties of various bearing materials in or near the boundary region. Discussions made in this paper are primarily based on the figures where the frictional force and the kinetic coefficient of friction are plotted against the load.

1. Introduction

Although the various investigations have been made of the properties regarding the kinetic friction in or near the boundary region, most of their results are deduced from the frictional phenomena respecting to a very small contacting area using the pure and special lubricants.

Our experimental works were appointed to frictional properties of relatively wide surface under the heavy load using available bearing metals and mineral oils, and we paid more attention to the discussion of the following three terms:

a) variations of frictional forces with loads and rubbing speeds (especially, the transition point from mixed to boundary friction),

b) variations of frictional coefficients with loads and speeds,

c) relations between the kinetic coefficient of friction and the temperature near the contact region.

Similar experimental works[1),2)] have been done for the purpose of determining how various factors influence on the kinetic friction in or near the boundary region, and the results of our research fundamentally coincided with their results.

Friction measurements in the extensive combinations of bearing metals and lubricating oils have revealed that

a) there is the unstable region in the latter parts of the mixed region regarding the kinetic coefficient of friction,

b) differences in the frictional properties among various materials increase with loads and speeds,

c) the rate of introduction of oils into rubbing surfaces and the strength of oil films at elevated temperature have the great influences on the boundary friction.

Next, from the results of investigating the wear process, it was revealed that the wear volume is directly proportional to the sliding distance and the load as the whole, and that the

* Department of Mechanical Engineering, College of Engineering
** Faculty of Technology, Kyoto University

effect of speed being equivalent to the effect of temperature has the intimate relation to the formation of oxide films on the worn surface.

2. Heavy Load Friction Tester

2.1 Apparatus

The schematic diagram of apparatus is shown in Fig. 1. Loads applied with the double lever mechanism can be changed from 50 Kg to 600 Kg. An upper specimen is rotated with the 3-phases induction motor (7.5 HP), and the number of revolutions is reduced through two pairs of Vie pulleys and one pair of bevel gears. Another specimen is fixed on the disk below, and the frictional moment acting on its rubbing surface is sustained by the spring balance through the pulley attached to the lower part of the axis of the disk.

Although the readings of the spring balance include values corresponding to the moment caused by the frictional resistance of the thrust ball bearing supporting the disk and the flexural resistance of the wire connecting the pulley with the spring balance, these values need not be regarded for the purpose of considering the relative variations of the frictional force. Rubbing surfaces are dipped into the mineral oil within the basin mounted on the disk, and the oil is circulated through the path shown in Fig. 1.

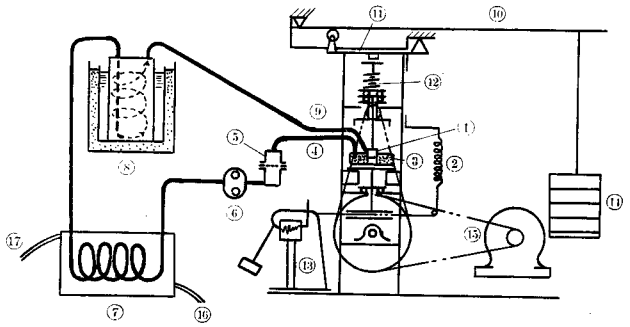

Fig. 1 Schematic diagram of tester

① Specimens
② Spring balance
③ Oil basin
④ Suction pipe
⑤ Oil filter
⑥ Gear pump
⑦ Thermostat (1st step)
⑧ Thermostat (2nd step)
⑨ Ejector
⑩ Lever (15:1)
⑪ Lever (4:1)
⑫ Level controller
⑬ Self-recorder
⑭ Weights (Max. 120 kg)
⑮ Motor
⑯ Cooling water inlet
⑰ Cooling water outlet

2.2 Conditions of Measurements

(1) Materials and shapes of specimens

The specimens of the types A, B and C were used in our experiment, whose shapes and dimentions are given in Fig. 2. The type C was the upper specimen made of mild steel (0.22% C), and A or B was used as the lower stationary one.

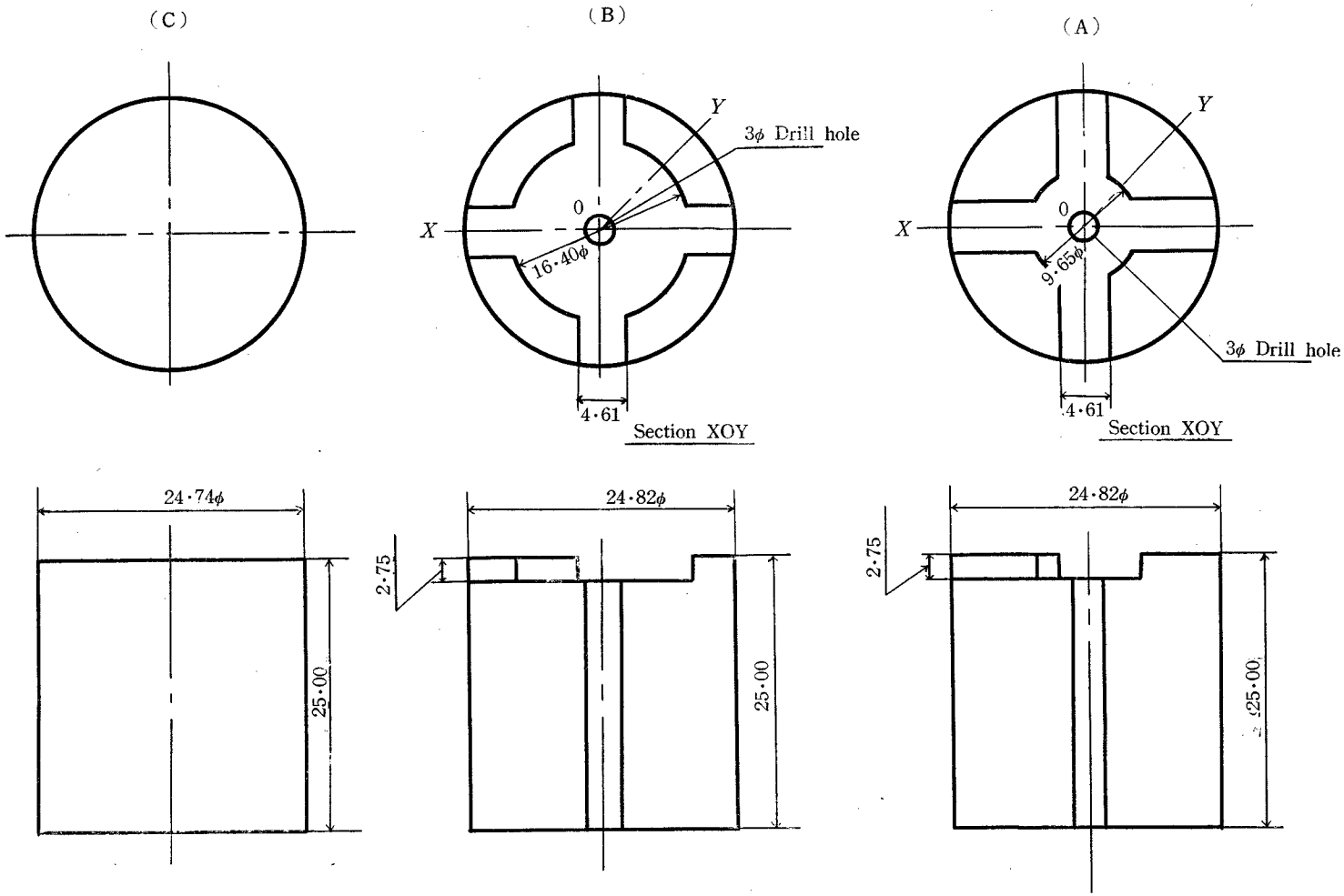

Fig. 2 Shapes of specimens

Crossed grooves and the circular cavity were machined on the surface of the lower specimen in order to make easy to introduce the lubricating oil into the interface of specimens.

The following metals were used as the lower specimens:

a) copper alloys

brass (6:4), gun metal, phosphorous bronze, alminum bronze, lead bronze, high strength brass (TM-1), berylium copper (BC-1).

b) ferrous materials

mild steel (S 22 C), cast iron (pearlitic structure), oil impregnated grown cast iron.

Compositions of copper alloys are listed on Table 1. The grown cast iron has the porous

Table 1 Compositions of copper alloys

Classification	% in weight					
6:4 Brass	Sn ·····	0.74	Pb ·····	2.80	Cu ·····	60.75
	Fe ·····	0.12	P ·····	——	Zn ·····	R
Gun metal	Sn ·····	4.49	Pb ·····	4.56	Cu ·····	R
	Fe ·····	0.05	P ·····	——	Zn ·····	4.03
Phosphorous bronze	Sn ·····	6.39	Cu ·····	R	P ·····	0.204
Alminum bronge	Al ·····	9.49	Ni ·····	2.59	Fe ·····	3.29
	Zn ·····	0.82	Mn ·····	0.97	Cu ·····	82.47
	Si ·····	0.08	C ·····	0.02		
Lead bronge—No. 1	Sn ·····	9.93	Pb ·····	12.23	Cu ·····	76.99
	Zn ·····	0.16	Ni ·····	0.09	Si ·····	0.03
	C ·····	0.03	Fe ·····	0.02		
Lead bronge—No. 2 (Isoled Bronze)	Sn ·····	10	Pb ·····	10	Cu ·····	R
High strength brass (TM—1)	Sn ·····	0.1~1.0	Pb ·····	0.1~1.0	Cu ·····	55~62
	Fe ·····	1.0~2.0	P ·····	0.1~1.0	Zn ·····	33~37
	Al ·····	0.1~1.0	Mn ·····	2~4	Fe ·····	0.2
Berylium copper (BC—1)	Be ·····	2.04	Co ·····	0.24	Si ·····	0.03
	Cu ·····	R				

structure due to being grown grains of the silicon riched grey pig iron, which is used as the oil impregnated bearing material.

(2) Load and rubbing speed

Load applied on the contact area was increased on the stepped wise such as the product of the load and the measuring time was nearly constant.

(3) Finish and preparation of surfaces

Surfaces of the specimens were prepared by lapping with the 500 grade emery paper, and fitted on the tester after cleaning by benzine and acetone. Then, the specimens were run at least one hour under the lowest load and speed in the series of this test until the vibration of the index of the spring balance almost ceased.

After the running-in drive, the surfaces were again lapped, and such procedures were

repeated until the surfaces came into uniform contact.

(4) Lubricating oils and their temperature

Properties of lubricating oils, especially their viscosities, vary remarkably with temperature, so that the temperature of oils were kept at 20°C±2°C by the oil circulating system shown in Fig. 1 to minimize the effect of temperature.

Of course, this temperature does not mean the value near the contact region, but the mean value of the oil temperature within the basin.

Types of lubricating oils (Maruzen Oil Company) used in this experiment were as follows:

♯120 machine oil (viscosity: C.S., 50°C, 29.5)
♯160 machine oil (viscosity: C.S., 50°C, 39.6)
Swalub S 700 oil (viscosity: C.S., 37.8°C, 155)
Swalub RO 700 oil (viscosity: C.S., 37.8°C, 145)
Swalub S 1400 oil (viscosity: C.S., 37.8°C, 302.2),

where Swalub S-series oils are pure mineral oils, and the Swalub RO 700 oil is added the oiliness additive, the anticorrosive and the antioxidizer on the Swalub S 700 as the base oil.

2.3 Experimental Techniques

(1) Frictional force

The readings of the spring balance were recorded at the regular intervals (every five minutes for the long intervals, and every two or three minutes for the short ones), from which frictional forces acting on the rubbing surface of the lower specimen were calculated using the following equations. That is, in Fig. 3 the rubbing area of the lower specimen will be expressed as

$$A=\int_{r_1}^{r_2}2r\left(\pi-4\sin^{-1}\frac{t}{r}\right)dr$$
$$=\pi(r_2^2-r_1^2)-4t(\sqrt{r_2^2-t^2}-\sqrt{r_1^2-t^2})$$
$$-4\left(r_2^2\sin^{-1}\frac{t}{r_2}-r_1^2\sin^{-1}\frac{t}{r_1}\right). \qquad (1)$$

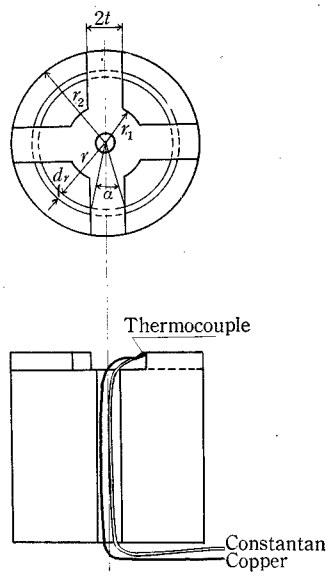

Fig. 3

From the assumption of uniformly distributed pressure, the frictional force is given by

$$F=\frac{3}{2}\frac{TRA}{\pi(r_2^3-r_1^3)-2t\{r_2\sqrt{r_2^2-t^2}-r_1\sqrt{r_1^2-t^2}+t^2\log(r_2+\sqrt{r_2^2-t^2})-t^2\log(r_1+\sqrt{r_1^2-t^2})\}}, \qquad (2)$$

where T is the reading of the balance, and R the mean radius of the pulley fixed on the axis of the disk.

Substituting eq. (1) in eq. (2), we have

$$F=\frac{3}{2}\frac{TR\left\{\pi(r_2^2-r_1^2)-4t(\sqrt{r_2^2-t^2}-\sqrt{r_1^2-t^2}-4\left(r_2^2\sin^{-1}\frac{t}{r_2}-r_1^2\sin^{-1}\frac{t}{r_1}\right)\right\}}{\pi(r_2^3-r_1^3)-2t\{r_2\sqrt{r_2^2-t^2}-r_1\sqrt{r_1^2-t^2}+t^2\log(r_2+\sqrt{r_2^2-t^2})-t^2\log(r_1+\sqrt{r_1^2-t^2})\}}. \quad (3)$$

Hence, the mean value of the coefficient of the kinetic friction μ is obtained from the equation of $\mu=F/P$.

(2) Temperature of the lubricating oil

We took measure of the mean temperature of oil within the basin and the temperature at the position being close to the region of contact. The temperature of oil within the basin was kept at $20°\pm2°C$ with the circulating system shown in Fig. 1, but the case that the mean temperature could be held by no means at 20°C was occasionally experienced especially at heavy loads and high rubbing speeds.

The temperature near the region of contact was measured at the position shown in Fig. 2 with the thermocouple led through the hole drilled along the center axis of the stationary specimen.

(3) Wear volume

Changes in weight and hight of the specimen of the type A were measured every twenty minutes for the revolutions of 47 r.p.m. and ten minutes for 95 r.p.m. after cleaning with benzine and acetone, and the same method was adopted for the type B specimen. However, for the materials having the tendency of absorbing oils, such as the pearlitic cast iron and the gun metal having small blow holes, losses in weight did not mean materials removed, so that the wear volume was calculated on the basis of the losses in height.

(4) Properties of worn surfaces

Properties of the rubbing surfaces were inspected with the Shore Hardness Tester and the SQ Meter (Surface Quality Meter).[3] The SQ Meter was tried to use for the purpose of the quantitative comparison of worn surfaces by the value named SQ which indicates the combined values of roughness and the metallographical properties.

3. Variations of Frictional Properties with Pressure

Shapes of specimens used in this experiment have already been shown in Fig. 2, where the rubbing surfaces of specimens of the type A have the similar forms to the Mitchell's Thrust Bearing, but oil wedges on a large scale can scarcely be established between mating surfaces during revolution.

A few papers have been published on the properties of the boundary friction referring to relatively wide areas under the heavy load (above 200 Kg/cm^2), so our experiment has been done under the conditions of the pressure above 180 Kg/cm^2 applied on the flat area of 2.75 cm^2 and 2 cm^2. As the #160 machine oil and the Swalub S 700 oil were used for the most kinds of materials, we wish to discuss the characteristics for these oils first of all. Following discussions are mainly made for the experimental results with regard to the specimens of the type A, but believed to hold true for another contact area such as the

type B.

3.1 Common properties among materials tested

From Figs. 4 and 5, it will be found that the frictional force/load curves change their tendencies at the loads between 1000 Kg and 2000 Kg. That is, the regions below these loads (the critical loads) are consist of mixed conditions of the fluid and the boundary lubrication, while the regions above the critical loads belong mostly to the boundry lubrication. The former is called the mixed region, and the latter the boundary region.

The shapes of the curves for the boundary regions are analogous to the dry friction, which is the characteristic of the materials of the specimens. While, the remarkable tendency shown in curves of the kinetic coefficient of friction/load is that they have two

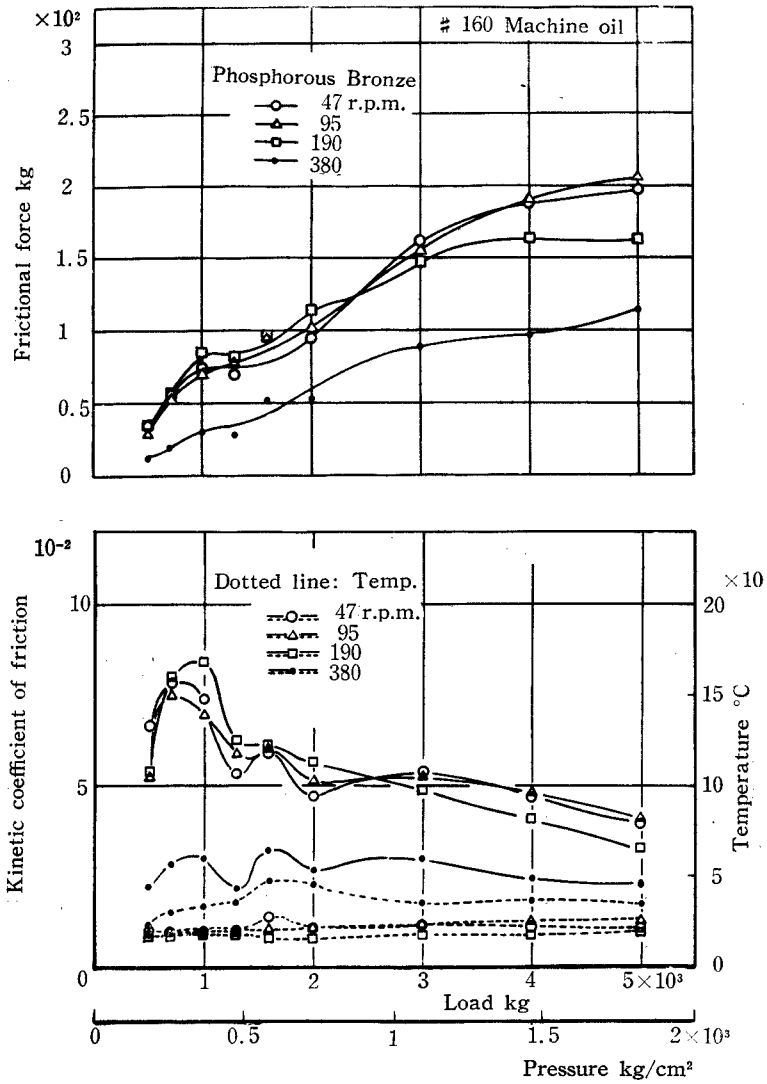

Fig. 4 Friction, kinetic coefficient of friction and temperature of contact region versus load curves.

vertexes in the mixed regions.

The existences of these points will be explained to be the result that the equilibrium condition between the strength of boundary oil films and the rate of the frictional heating varies instably with loads. That is, the real area of contact gradually increases with pressure, besides, reduction in thicknesses of oil films and increase in viscosities as well occure with further increasing pressure, which yield temporarily the high coefficient of friction that is displayed as the first maximum value. Exceeding this point, the excess frictional heating reduces moderately the shear strength of oil films and welds, so that the kinetic coefficient of friction begins to decrease due to the additional effect of the thermal expansion of the thickness of oil films as well.

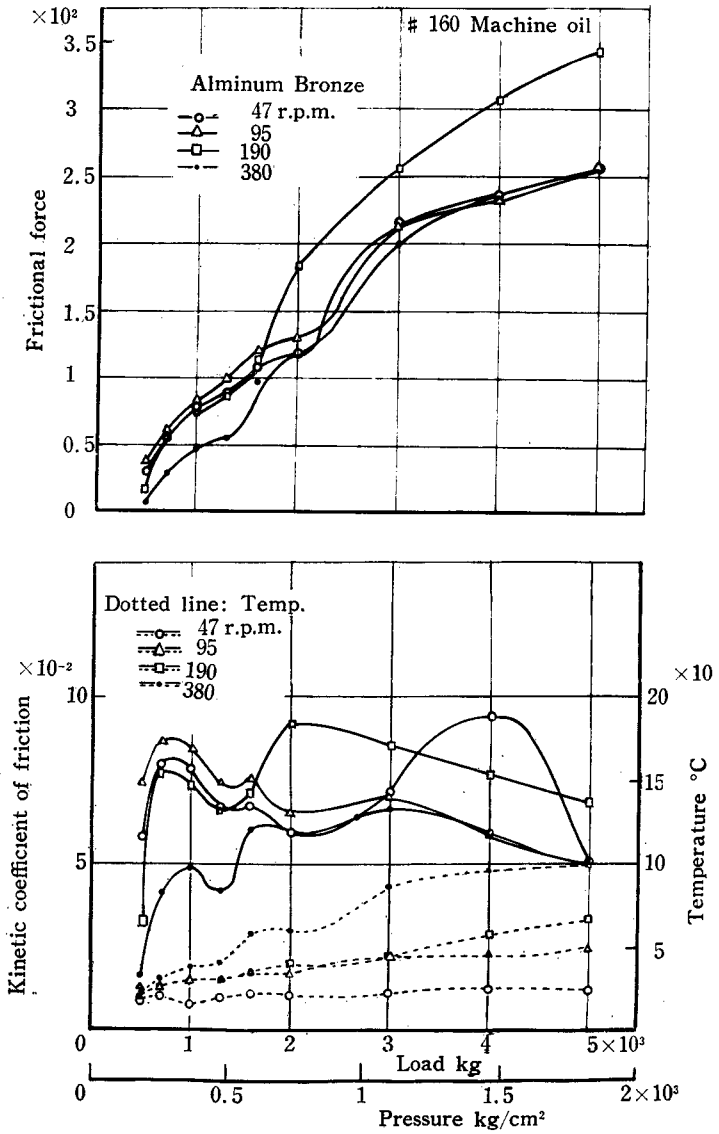

Fig. 5

However, increasing the load much more, the similar process succeed again on a smaller scale, and thereafter, the trend of curves shifts to the boundary region.

Now, the above interpretation was deduced from the macroscopic observation of the kinetic coefficient of friction, so that minute variations in the coefficient of friction might have been observed within subdivided regions of loads.

Next, considering the behavior in the boundary region, it will be seen from Fig. 4 that the frictional force increases markedly above the critical point, and then gradually reduces the rate of increase toward the domain of heavy loads, while the kinetic coefficient of friction indicating the minimum value near the critical point gradually increases for a while, and then decreases or remains nearly constant except for the case of seizure.

Above phenomena will be explained as follows. This is, the rate of frictional heating near the critical point becomes to be appreciably large, since the rubbing surfaces near the critical point display the condition of the boundary lubrication for the large part. Hence, the rate of increase in the frictional force reduces owing to the reduction of the strength of the boundary layer, accordingly the corresponding value of the kinetic coefficient of friction shows the minimum value at this point. Above the critical point, i.e., in the boundary region, the thickness of the layer reduces and the proportion of loads carried by oil films decreases with increasing loads, so that the frictional force increases remarkedly owing to the "dry friction effect".

However, the rate of increase in the frictional force begins to reduce within the domain above the certain load (about 3000 Kg), because the increase of the real area of contact becomes to be dull, and the shear strength of the material reduces due to frictional heating. Besides, the solid lubricants added in materials and the oxide film formed on the rubbing surfaces contribute to the anti-friction effects in the domain of very high load. Provided that the material does not contain anti-friction elements, or the effects of oxide films are not remarkable, the rubbing surfaces can fall into the condition of seizure.

Strength of oil films which is generally proportional to the viscosity of oil has a great effect on seizure too, but experimental results revealed that the higher viscosity had not always the more superior effect.

The common properties above mentioned are shown in Figs. 6~12, which display together the curves of frictional force/load for various materials with five kinds of lubricating oils.

3.2 Frictional properties of various metals for the specified lubricating oil

Fig. 6 shows an example of frictional force (the kinetic coefficient of friction)/load curves for the Swalub S 700 oil whose quality is superior to the #160 machine oil. The tendency is similar to Fig. 4 or Fig. 5, but frictional forces and kinetic coefficients of friction reduce appreciablly as a whole, and variations of coefficients of friction become considerably small. In Figs. 7~13, friction/load curves for various materials using five kinds of lubricating oils are shown in order to compare differences in frictional properties for the natures of oils and rubbing speeds. Firstly, in Fig. 7 for the #160 machine oil, it is shown that curves except for (1) and (4) show a good agreement up to the load of 2000 Kg, which

indicates that the amount of fluid lubrication is relatively large within the mixed region at the revolution of 47 r.p.m..

Tendencies of the curves (1) and (4) are analogous to each other, but the frictional force increases considerably from the early stage. This is due to the fact that the grown cast iron for the curve (1) was tested by the method of drop feed, and that the "dry friction" effect on the 6:4 brass is already remarkable at light loads owing to the low shearing strength of the material and its marked reduction at the elevated temperature.

Within the boundary region (above the load of 2000 Kg), tendencies and positions of curves for various metals differ respectively, which can be classified into three groupes as follows:

a) High friction groupe .....(1), (4), (10)

b) Moderate friction groupe .....(2), (3), (6)

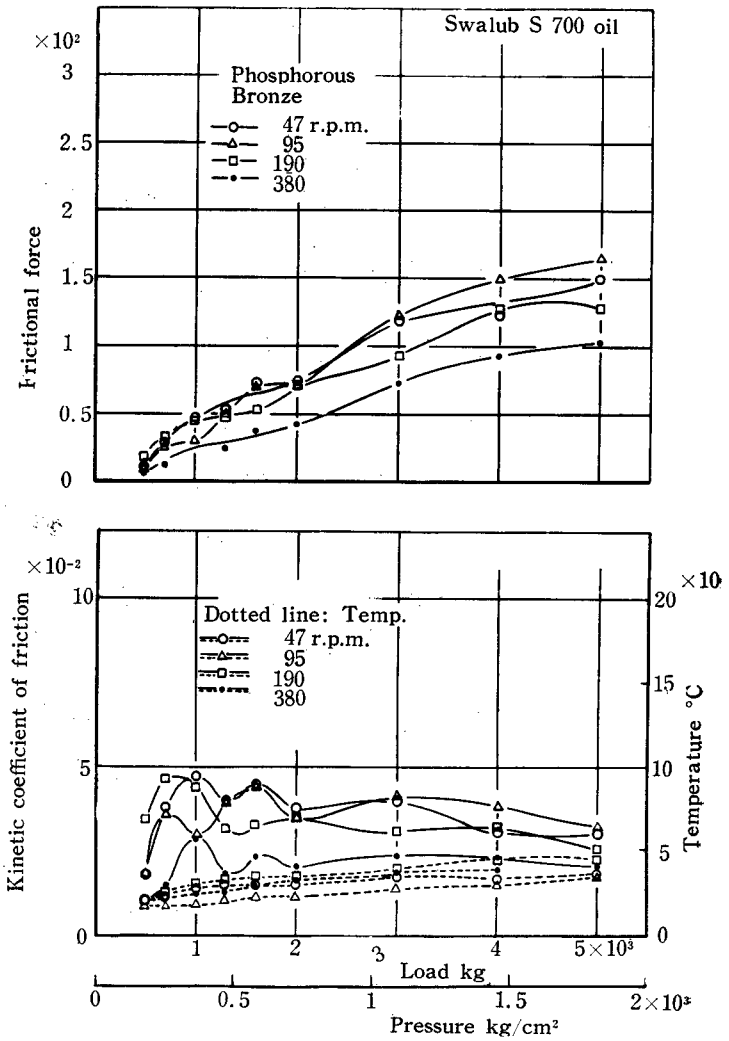

Fig. 6

c) Low friction groupe .....(5), (7), (8), (9)

Tendencies above mentioned scarcely change at 95 r.p.m., but seizures of the grown cast iron and the 6:4 brass occur at the earlier stages. However, as shown in Fig. 8, differences among materials grow strikingly as the rubbing speed becomes higher. That is, the curve (5) for the phosphorous bronze and the curve (7) for the lead bronze become to be located at lower positions, but the other curves climb to higher positions on the contrary. Among them the behavior of the high strength brass (9) is distinguished in the latter half of the boundary region.

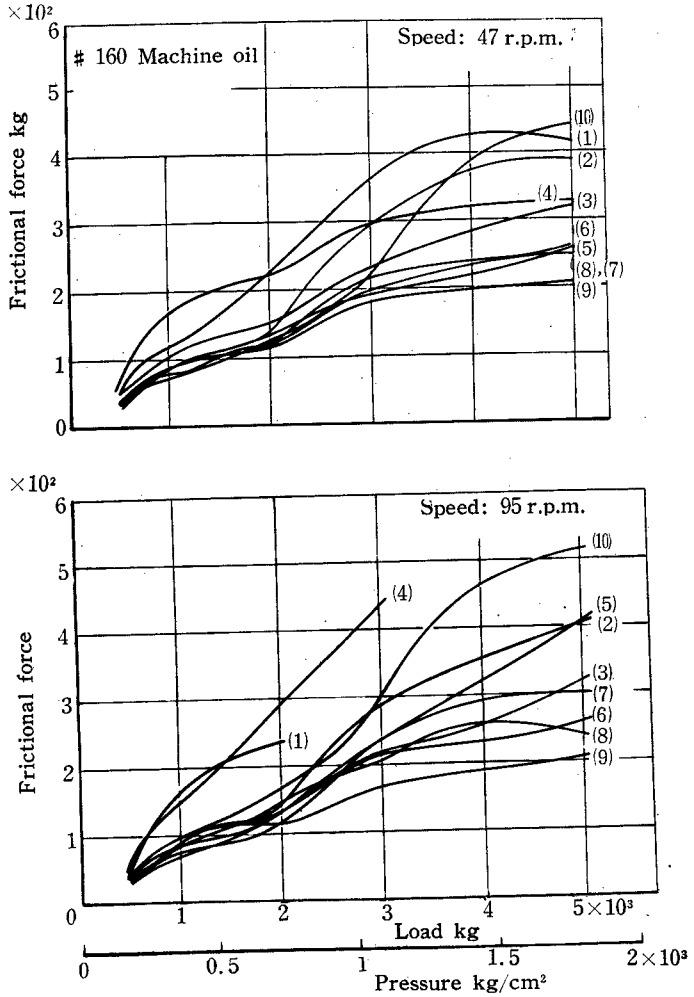

Fig. 7 Frictional force versus load curves for various metals. Lubricating oil: #160 Machine oil.

(1) Grown cast iron, (2) Pearlitic cast iron,
(3) Gun metal, (4) 6:4 Brass,
(5) Phosphorous bronge, (6) Alminum bronze,
(7) Lead bronze No. 1, (8) Lead bronze No. 2,
(9) High strength brass, (10) Berylium copper

At the highest speed in this experiment, i.e., at 380 r.p.m., frictional forces for bronzes reduce, among which the phosphorous bronze shows especially stable and superior performance, but materials other than bronzes fall into the conditions of seizure.

Secondary, from the curves for the Swalub S 700 oil shown in Figs. 9 and 10, it is revealed that tendencies are analogous, but much superior than the #160 machine oil for the regions of high loads and speeds. Besides, for the Swalub RO 700 oil, frictional forces reduce further except for the phosphorous bronze, and the reduction in friction is marked for the high speed as shown in Fig. 11.

Such undesirable effect of the Swalub RO 700 oil on the phosphorous bronze will possibly be caused by the anti-oxidizer or the anti-corrosive included in the oil. That is, these additives seem to have repressed the formation of oxide films as anti-frictions.

Finally, from the curves for the #120 machine oil (Fig. 12) and the Swalub S 1400

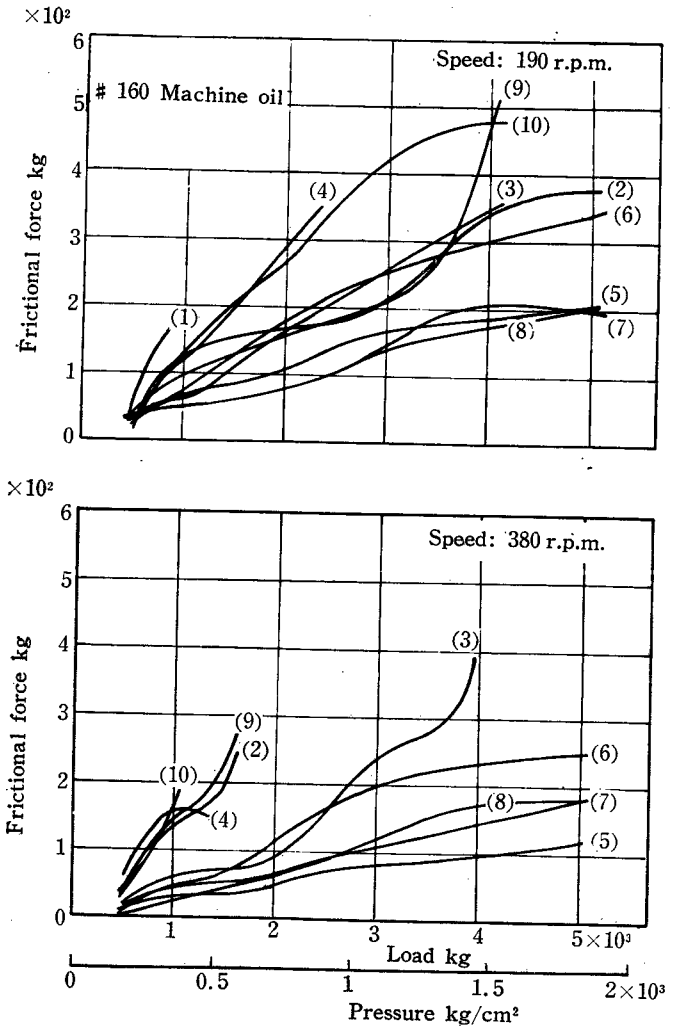

Fig. 8 Frictional force vs. load curves. Lubricating oil: #160 Machine oil.

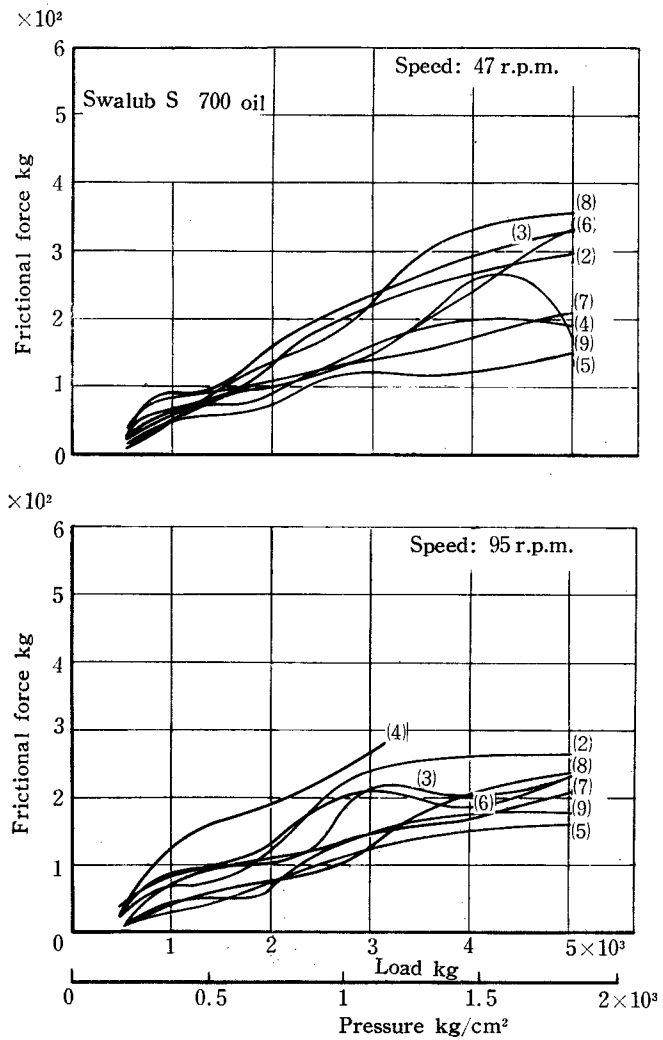

Fig. 9 Frictional force vs. load curves. Lubricating oil: Swalub S 700 oil.

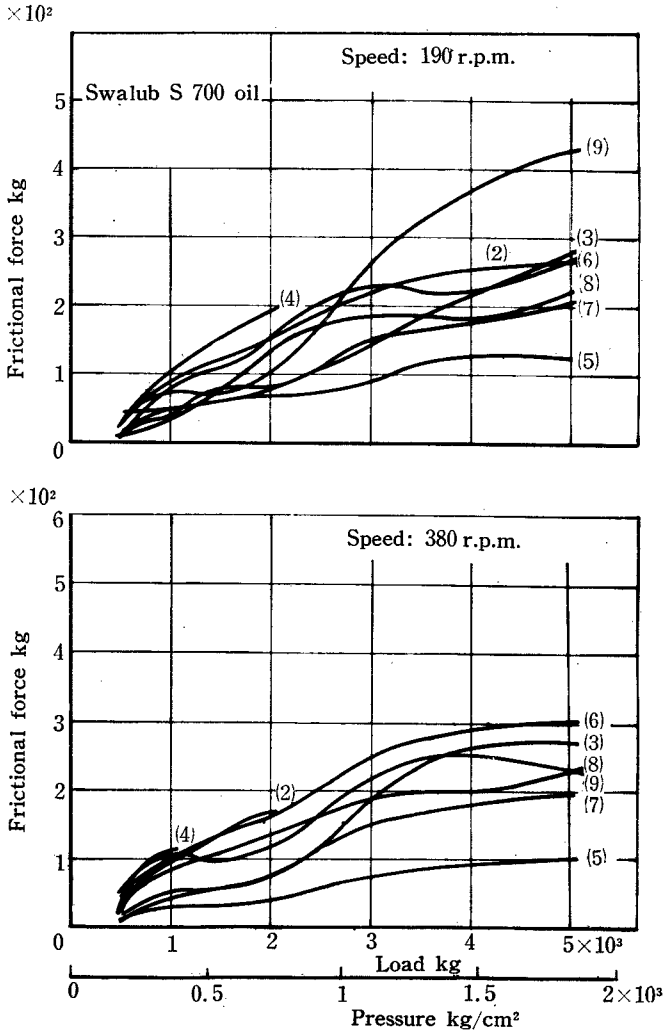

Fig. 10 Frictional force vs. load curves. Lubricating oil: Swalub S 700 oil.

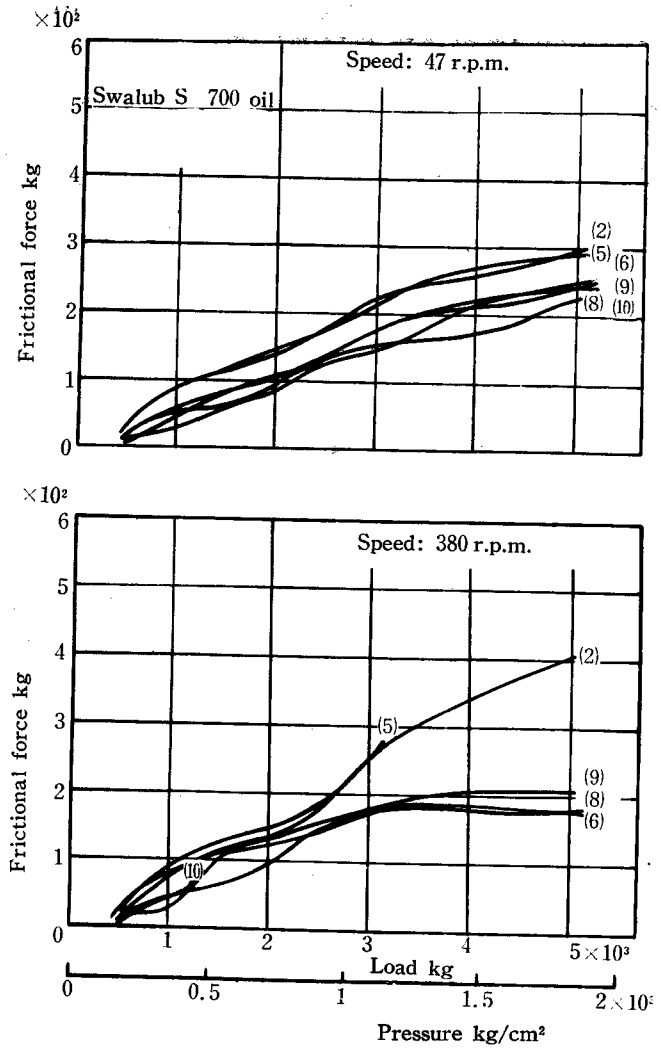

Fig. 11 Frictional force vs. load curves. Lubricating oil: Swalub RO 700 oil.

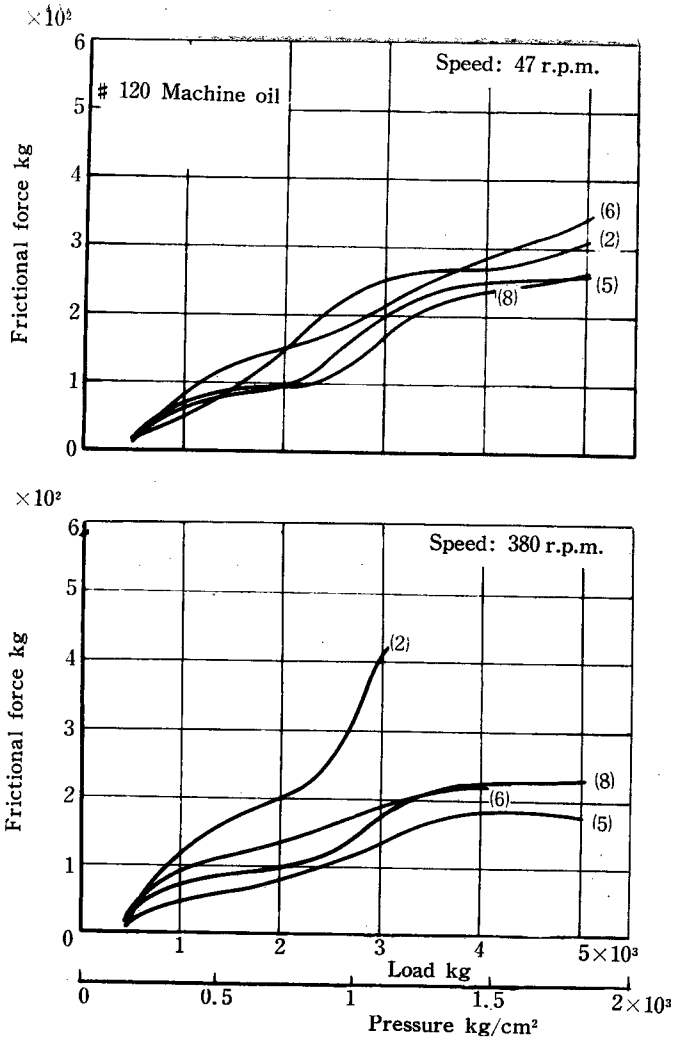

Fig. 12 Frictional force vs. load curves. Lubricating oil: #120 Machine oil.

oil (Fig. 13), it will be found that superiority of bronzes to the pearlitic cast iron becomes distinct at high speed. However, bronzes is not always superior to the cast iron over all regions at low speed. For example, in the upper diagram of Fig. 12, differences can scarcely be recognized, while the upper diagram of Fig. 13 shows that the pearlitic cast iron is inferior to bronzes in the mixed region, but reverse its trend in the boundary region.

We shall leave the discussion of these results to the following section, but the rate of introduction of oil and the temperature due to frictional heating are supposed to have serious effects.

3.3 Lubricating properties of various oils

(1) For bronzes

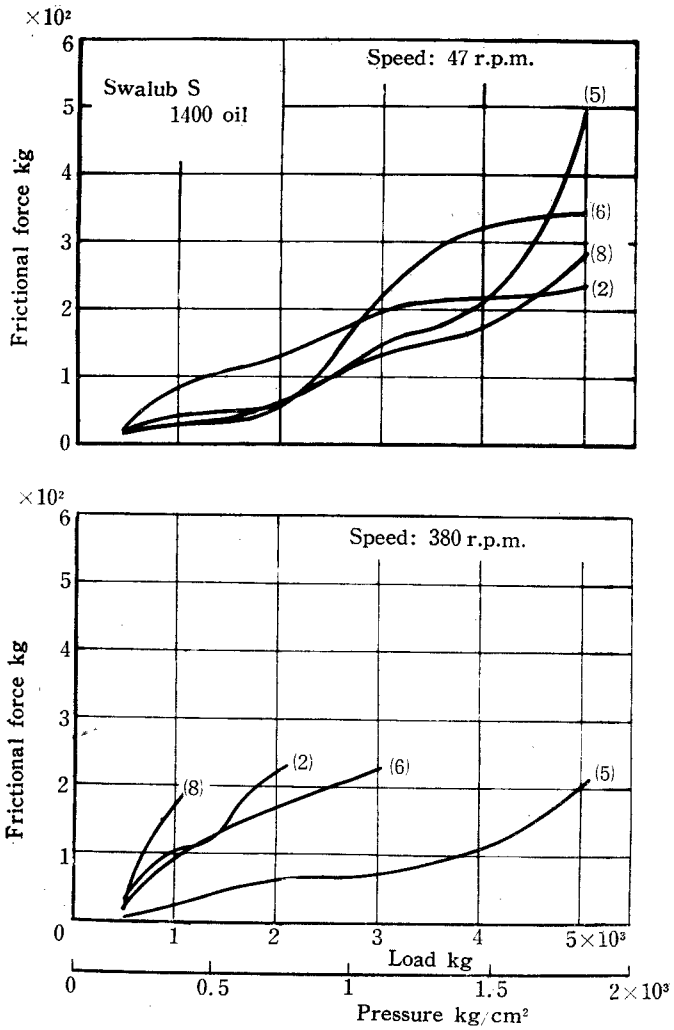

Fig. 13 Frictional force vs. load curves.
Lubricating oil: Swalub S 1400 oil.

As shown in Figs. 14~16, frictional forces are generally reversely proportional to viscosities for low speeds in the mixed region, but tendencies are uncertain for high speeds in the mixed region or in the boundary region.

However, frictional forces for the Swalub S 1400 oil (high viscosity) increase markedly in the boundary region despite of showing lower values in the mixed region, and indicate the condition of seizure at relatively light loads for high speeds (see also Fig. 13). It is largely due to frictional heating and the rate of introduction of oil into the interface of the specimens.

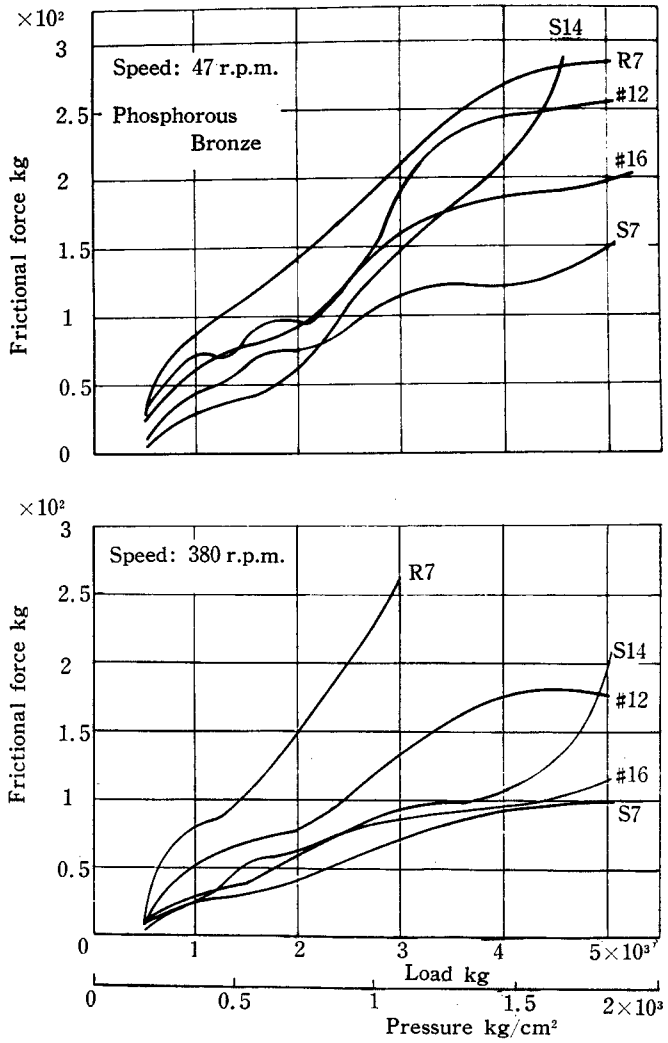

Fig. 14 Frictional force vs. load for different oils.
Material: Phosphorous bronze.

#12 ····· #120 Machine oil.
#16 ····· #160 Machine oil.
S 7 ····· Swalub S 700 oil,
R 7 ····· Swalub RO 700 oil,
S 14 ····· Swalub S 1400 oil.

That is, the rate of introduction increases with increasing speeds and the viscosity of oil reduces to a medium value due to moderately frictional heating in the region of low loads.

The rate of introduction, however, reduces with loads due to the spreading of real areas of contact, so that high speeds under the heavy load bring about considerable reduction of the shear strength of materials and the widespread break-down of oil films owing to severely frictional heating.

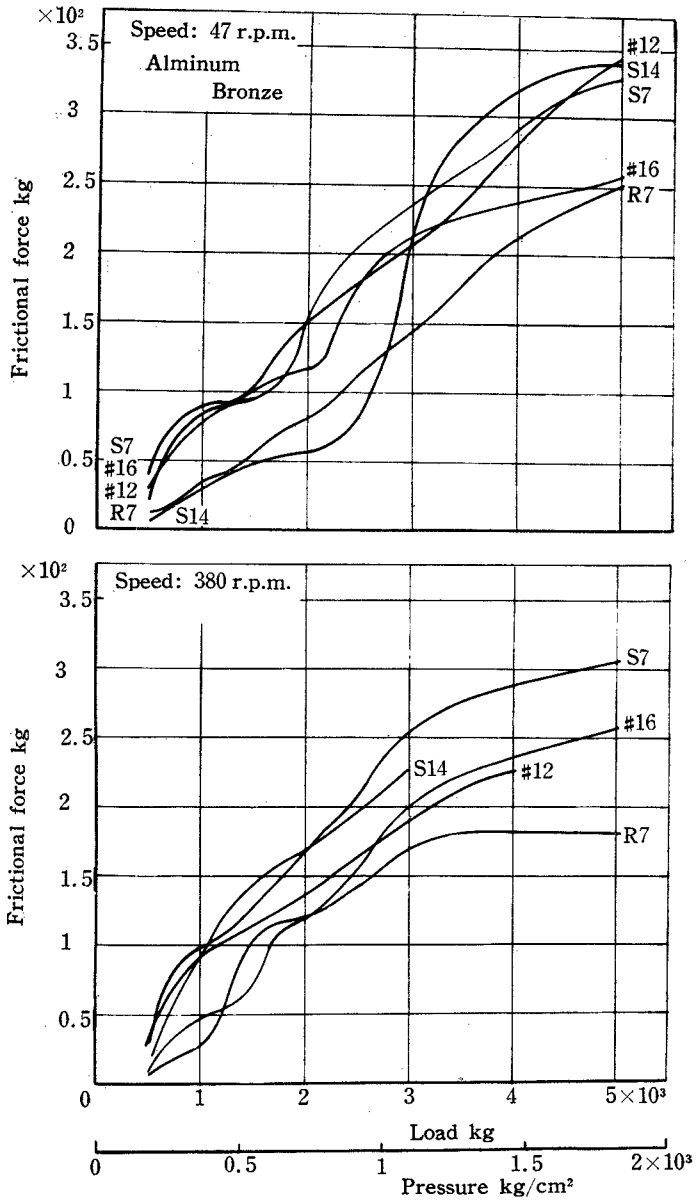

Fig. 15 Frictional force vs. load curves.
Material: Alminum bronze

(2) For pearlitic cast iron

It will be found in the upper diagram of Fig. 17 that the frictional force being proportional to the viscosity of oil in the mixed region almost reverses its tendency in the boundary region at low speeds, and that other oils except for the Swalub RO 700 oil give rise to seizure in the earlier stage, whose results will probably be caused by the coarse structure and the poor thermal conductivity of the pearlitic cast iron. That is, fluid lubricating films partially formed between the sliding surfaces are relatively thick and occupy the large part of the mixed region, hence the frictional force is nearly proportional to the viscosity of oil at low speeds.

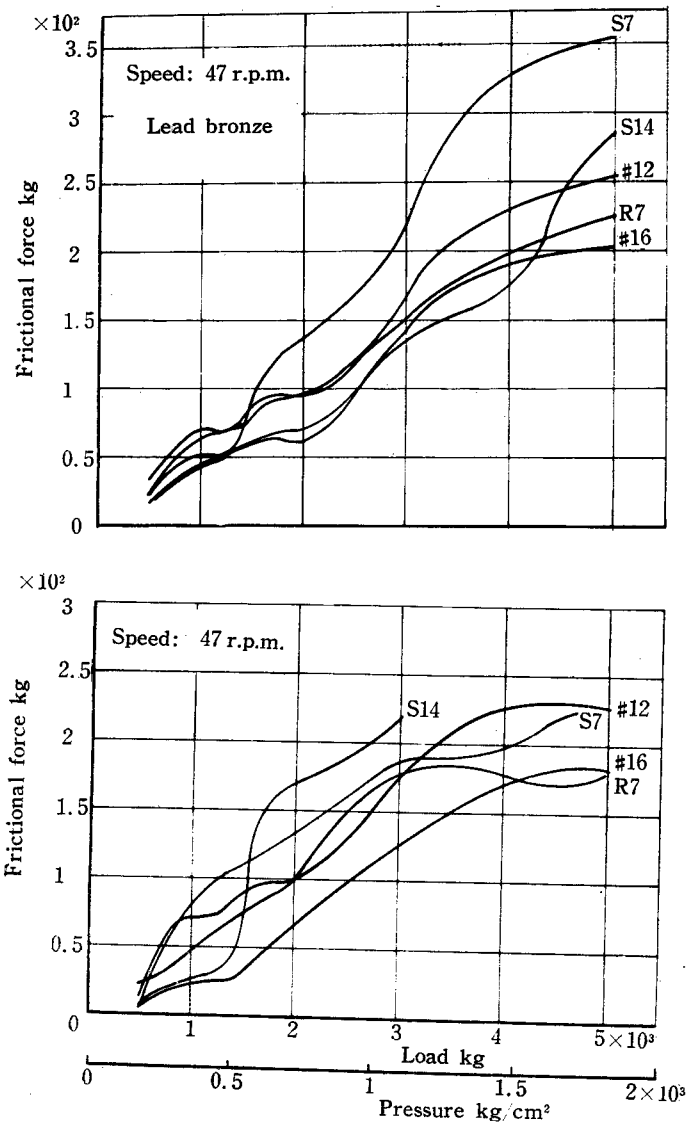

Fig. 16 Frictional force vs. load curves.
Material: Lead bronze.

While, in the boundary region, flaky graphites separated from the worn surface act as the solid lubricant on the real area of contact, and oils staying in pits produced by the separation of graphites help to form the boundary oil films, so that the frictional forces for the high viscosity oil (generally high strength of oil film) become lower at low speeds. At high speeds, however, the break-down of the boundary oil films on a large scale are caused by severely frictional heating due to the high dry friction and poor heat conductivity of the materials, and the microscopic effect of oils in pits as the thermal insulator.

Consequently, frictional forces are held on high values even in the mixed region, and the seizure occurs early as shown in the lower diagram of Fig. 17 (see also Figs. 12 and 13).

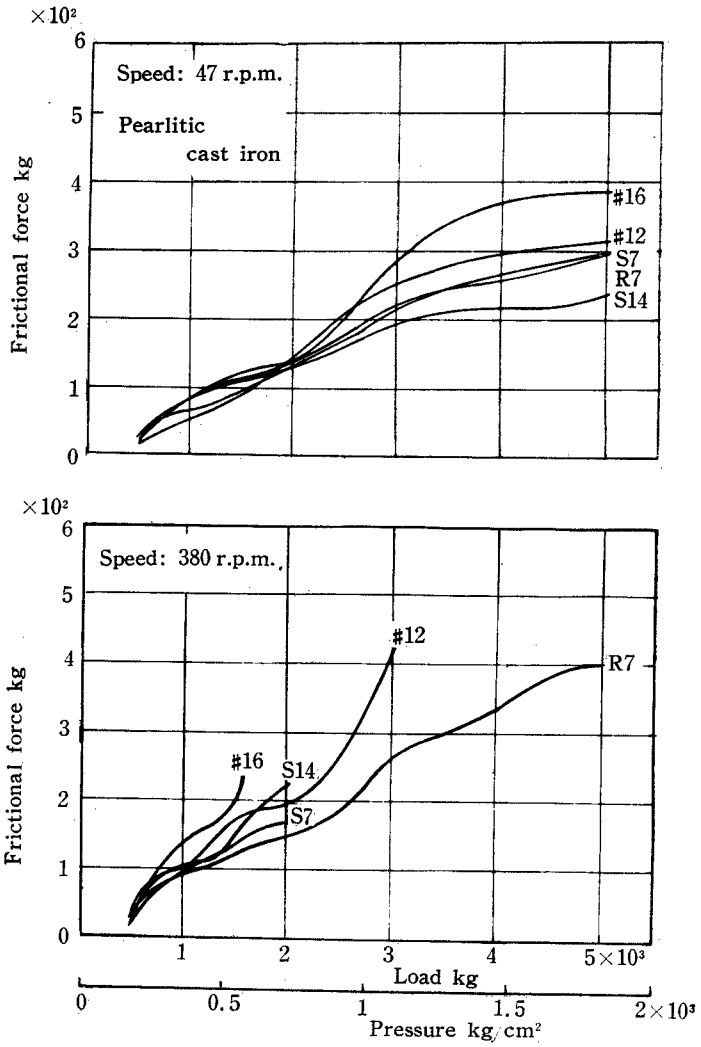

Fig. 17 Frictional force vs. load curves.
Material: Pearlitic cast iron.

(3) Effects of the oiliness additive

Comparing Fig. 11 with Fig. 10, or taking notice of the curves for the Swalub RO 700 oil in Figs. 15~17, frictional forces decrease by adding the oiliness additives on the whole. Besides, it was clearly recognized that the oiliness additives would contribute to strengthen oil films at elevated temperature, because of their marked effects especially at heavy loads (in the boundary region) and high speeds. Again, it is the interesting phenomena that curves for the phosphorous bronze in Fig. 14 indicate the reversal in their trends, the reasons of which have already been mentioned (see 3.2).

4. Conclusion

From the experimental results described above, we confirmed the noticeable behavior of the coefficient of kinetic friction within the mixed region.

Then, discussing the influences of the properties of oils and sliding speeds, it was revealed that differences in frictional properties existing among materials tested would become greater with sliding speeds, and that the rate of oil introduction and frictional heating might have the striking effects on the frictional characteristics.

(to be continued)

References

1) P. G. Forrester, Proc. Roy. Soc., **A 187**, 439 (1946).
2) R. L. Lening. J. ASLE, Dec., 575 (1960).
3) S. Yamasaki, J. Soc. Precis. Mech. Japan, **Vol. 20**, No. 4, 130 (1954).